BIOCHEMISTRY

 Volume 44, Number 25 June 28, 2005

Articles

The Internal Cavity of the Staphylococcal α-Hemolysin Pore Accommodates ~175 Exogenous Amino Acid Residues†

Yuni Jung,‡ Stephen Cheley,‡ Orit Braha,§ and Hagan Bayley*,§

Department of Medical Biochemistry and Genetics, The Texas A&M University System Health Science Center, College Station, Texas 77843-1114, and Department of Chemistry, University of Oxford, Chemistry Research Laboratory, Mansfield Road, Oxford, OX1 3TA, United Kingdom

Received December 15, 2004; Revised Manuscript Received April 20, 2005

ABSTRACT: The cavity within the cap domain of the transmembrane staphylococcal α-hemolysin (αHL) pore is roughly a sphere of diameter ~45 Å (molecular surface volume ~ 39 500 Å^3). We tested the ability of the cavity to accommodate exogenous polypeptide chains. Concatemerized Gly/Ser-containing sequences ("loops", L; number of repeats = n; number of residues = $10n + 5$, $n = 0-21$) were inserted at a position located within the cavity of the fully assembled heptameric αHL pore. Homomeric pores containing 25 or less residues in each loop ($n \leq 2$) could be assembled. The pores were protease-resistant, indicating that they had been formed correctly, and produced currents in planar lipid bilayers. The pores showed an up to 70% reduction in unitary conductance, depending on the length of the inserted loop. Protease-resistant heteromeric pores containing wild-type (W) and L subunits were also assembled: when $n = 3$, up to five L subunits were tolerated; when $n = 4$, three L subunits were tolerated; and when $n = 5$ or 6, two L subunits were tolerated. For $n \geq 7$, only one L subunit was incorporated. As the inserted loop was lengthened, transient closures were observed in planar bilayer experiments with single pores. However, L_1W_6 pores with very long loops ($n = 14$ and 21) had unitary conductance values close to those of W_7, suggesting that the loop is extruded through the opening in the cap of the pore into the external medium. Further analysis of bilayer recordings and electrophoretic migration patterns indicates that the upper capacity of the cavity is ~175 amino acids. The findings suggest that small functional peptides or proteins might be assembled within the αHL pore.

The α-hemolysin (αHL)[1] pore is formed from an exotoxin secreted by *Staphylococcus aureus*. The pore has been useful for fundamental studies of membrane protein assembly and function. Furthermore, applications in biotechnology are

† Work at Texas A&M University was supported by DARPA, the DoD Tri-Service Technology Program, DOE, NASA, NIH, and ONR. H.B. is the holder of a Royal Society−Wolfson Research Merit Award. O.B. was supported by the Wellcome Trust.

* To whom correspondence should be addressed: Department of Chemistry, University of Oxford, Oxford, OX1 3TA, U.K. Telephone: +44-1865-285101. Fax: +44-1865-275708. E-mail: hagan.bayley@chem.ox.ac.uk.

‡ The Texas A&M University System Health Science Center.

§ University of Oxford.

[1] Abbreviations: αHL, staphylococcal α-hemolysin; IVTT, *in vitro* transcription and translation; L, the L (loop) subunits of αHL contain $10n + 5$ additional residues, where n is the number of decapeptide repeats, e.g., L25 contains two Gly/Ser-containing repeats plus 5 flanking residues for a total of 25 residues; LB, Luria−Bertani; MBSA solution, 10 mM MOPS at pH 7.4, 150 mM NaCl, and 1 mg/mL BSA, where MOPS is 4-morpholinepropanesulfonic acid and BSA is bovine serum albumin; MePEG-OPSS, monomethoxypoly(ethylene glycol)-*o*-pyridyl disulfide; PEG, poly(ethylene glycol); rRBCM, rabbit red blood cell membranes; W, wild-type αHL subunit.

10.1021/bi0473713 CCC: $30.25
Published on Web 06/04/2005

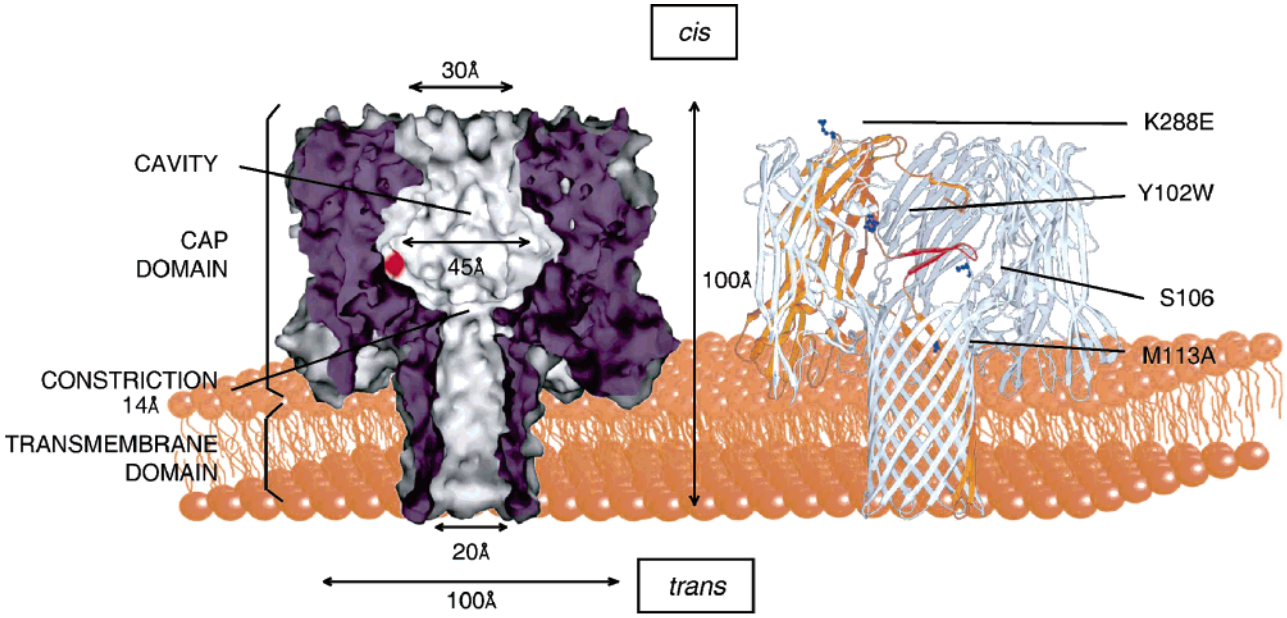

FIGURE 1: Structure of the αHL pore and a model of a loop-containing subunit. (Left) Transverse section through the heptameric pore [7AHL (*5*)] in a lipid bilayer. The widest region of the internal cavity is ~45 Å in diameter. The cavity is roughly spherical with a molecular surface volume of ~39 500 Å^3. One of the seven Ser residues at position 106 is shown in red. (Right) Section through the pore showing the locations of residue 106 and the mutations relevant to this work. In one of the subunits, a loop of 15 residues (red) has been inserted upstream of position 106.

emerging; e.g., engineered pores can used be as components of sensors (*1*) or to permeabilize cells for the introduction of cryoprotectants (*2*). The pore has also been used as a nanoreactor to observe covalent chemistry at the single-molecule level (*3*).

αHL is secreted as a monomeric water-soluble protein, which assembles into a heptameric pore on cell membranes (*4*). The pore comprises an extramembraneous cap domain and a transmembrane β barrel (Figure 1) (*5*). A water-filled channel runs through the pore along the axis of molecular symmetry (*6*). The diameter of the channel ranges from 45 Å for the widest region in the cap to 14 Å for the narrowest region, known as the constriction. The opening of the pore at the cis side of the bilayer measures 30 Å in diameter and on the trans side measures 20 Å in diameter (Figure 1). On the basis of the X-ray crystal structure of the pore, the molecular surface volume of the cavity within the cap domain is ~39 500 Å^3.

In previous work from this laboratory, the interior of the cap domain was chemically modified with monomethoxy-poly(ethylene glycol)-*o*-pyridyl disulfide (MePEG-OPSS) molecules (*7*). The cavity was able to tolerate the presence of one but not two poly(ethylene glycol) (PEG) chains of 5000 Da. Movements of the PEG within the lumen of individual pores could be detected by electrical recording. The PEG-containing αHL pore was further engineered for the detection of proteins in solution (*8*). After the placement of biotin on the untethered end of the PEG chain (3400 Da in this case), the modified αHL pore could capture proteins in the bulk solution (streptavidins or anti-biotin antibodies). After capture, the movement of the PEG within the pore was dampened, providing a characteristic signature for the binding events.

In the present work, we evaluate the use of genetic engineering, rather than targeted chemical modification, to place polymers within the lumen of the pore: in this case, loops comprising Gly/Ser-containing polypeptides. We estimate the capacity of the cavity to contain polypeptide sequences and examine the dynamics of the inserted loops. A long-term goal is to place small functional peptides or proteins within the αHL pore.

EXPERIMENTAL PROCEDURES

Construction of αHL Genes Containing Concatemeric DNA Sequences Encoding Internal Polypeptide Loops. Genes encoding αHL subunits with internal polypeptide loops (L) of various lengths were constructed in three steps: the introduction of unique restriction enzyme sites for cassette mutagenesis, the generation of repeat units, and the concatemerization of the repeats and insertion into the gene (Figure 2A). Unique *Msc*I and *Mlu*I sites were introduced into the central region of the αHL gene by a recombination-PCR protocol (*9*). Two sets of PCR were performed on the pT7-WT αHL template (*10*). The mutagenic primers were 5′-TCGATTGATACAAAAGAGTACGCGTCTACTTTAA-CTTATGGATTC-3′ (5′ half, sense) and 5′-TGTATCAATC-GAATTTCTTGGCCAGTAATCAGATATTTGAGCTAC-3′ (3′ half, antisense). The nonmutagenic primers were 5′-CAGAAGTGGTCCTGCAACTTTAT-3′ (5′ half, antisense) and 5′-ATAAAGTTGCAGGACCACTTCTG-3′ (3′ half, sense). The PCR products were mixed together and used to co-transform *Escherichia coli* XL10 Gold (Stratagene, La Jolla, CA). The cells were grown for 16 h on LB-ampicillin plates. *Mlu*I digestion was used to screen for the new *Msc*I- and *Mlu*I-containing plasmid (pT7-WM102). The entire αHL gene WM102 in pT7-WM102 was sequenced, and a fortuitous Lys-288→Glu mutation was discovered, which later proved useful for the separation of heteromeric pores (see the Results). To revert the latter mutation in WM102 and in the genes encoding the loop-containing mutants (see below), a gel-purified *Nde*I−*Mfe*I fragment from each construct was inserted into the pT7-WT αHL vector that had been prepared

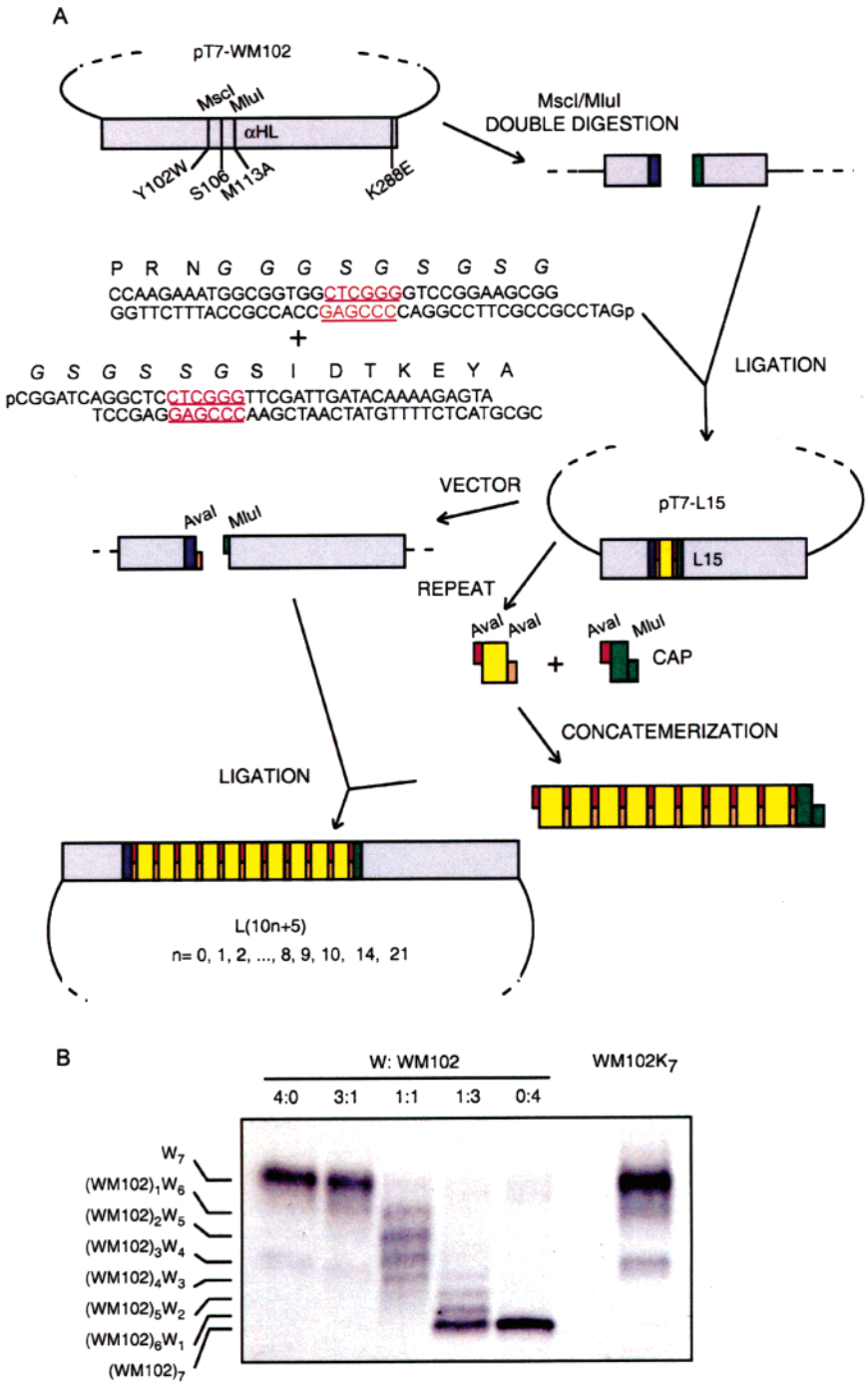

FIGURE 2: Construction of αHL genes containing concatemeric DNA sequences encoding internal polypeptide loops. (A) To introduce *Msc*I and *Mlu*I sites for cassette mutagenesis, Y102W and M113A mutations were introduced by PCR *in vivo* recombination. The K288E mutation was fortuitously generated during this process. The resulting vector, pT7-WM102, was digested with *Msc*I and *Mlu*I and then ligated with a synthetic duplex encoding PRN*GGGSGSGSGGSGSSG*SIDTKEYA. The italics indicate the inserted Gly/Ser-rich loop of mutant L15. The underlined red nucleotides indicate nonpalindromic *Ava*I sites. The repeat unit was purified after *Ava*I digestion of L15. Tandem ligation of the repeat was performed in the presence of unphosphorylated cap oligonucleotides to control concatenation (cap/repeat, 1:20). Concatemers were purified and ligated to a vector comprising the L15 plasmid from which the *Ava*I−*Mlu*I fragment had been removed. The nomenclature of the L subunits is L(10*n* + 5), where *n* is the number of repeat units. (B) Electrophoretic separation of heteromers formed from W αHL subunits and WM102 subunits. An autoradiogram of a 5% SDS−polyacrylamide gel is shown. Plasmids encoding W and WM102 subunits were mixed in various ratios (indicated above the lanes) for coupled IVTT in the presence of [^{35}S]-methionine and rRBCM. After translation, the washed membranes were solubilized in MBSA buffer, mixed with an equal volume of 2× Laemmli sample buffer, and subjected to electrophoresis without heating. The autoradiogram shows the electrophoretic ladders generated by the Lys-288→Glu mutation in the WM102 subunits. Homoheptamers formed by the revertant WM102K (Lys at position 288) are shown in the right-hand lane.

with the same restriction enzymes. All of the revertant genes were sequenced.

The loop-containing subunits (L) were designated by the length of inserted polypeptide chain (10*n* + 5, where *n* is the number of repeat units). The first loop-containing mutant, L15, was generated by ligation of two double-stranded oligonucleotides formed from the single strands 5′-CCAA-GAAAT*GGCGGTGGCTCGGGGTCCGGAAGCGG*-3′, 5′-

p*CGGATCAGGCTCCTCGGGT*TCGATTGATACAAAAG-AGTA-3′,5′-CGCGTACTCTTTTGTATCAATCGA*ACCCGAGGAGCCT*-3′, and 5′-p*GATCCGCCGCTTCCGGACCCCGAGCCACCGCC*ATTTCTTGG-3′ into the vector pT7-WM102 from which the central *Msc*I−*Mlu*I fragment had been removed (Figure 2A). This DNA encodes the amino acid sequence PRN*GGGSGSGSGGSGSSG*SIDTKEYA, where the exogenous Gly/Ser-rich sequence is in italic. The *Ava*I sites, which flank the repeat unit, are underlined in the oligonucleotide sequences.

A series of DNA concatemers was generated by tandem ligation of the purified repeat unit in the presence of "cap" oligonucleotides (Figure 2A). Head-to-tail oligomerization was ensured by the nonpalindromic *Ava*I sites flanking the repeat (*11*, *12*). The cap oligonucleotides served to control the length of the concatemers and to allow directional cloning without self-ligation (Figure 2A). A substantial amount of the 30-bp repeat unit (∼0.5 μg) was prepared by *Ava*I digestion (300 units) of the L15 plasmid (170 μg DNA, 37 °C for 16 h), followed by purification by polyacrylamide gel electrophoresis in Tris-borate-EDTA (TBE) buffer at pH 8.0. The cap sequences were 5′-TCGGGTTCGATTGATA-CAAAAGAGTA-3′ (sense) and 5′-CGCGTACTCTTTTG-TATCAATCGAAC-3′ (antisense), which encode *G*SIDT-KEYA. The initial Gly is a newly introduced residue. The remaining amino acids are from the wild-type sequence (residues 106−113) except for the final Ala, which corresponds to the mutation Met-113→Ala (Figure 2A). The cap duplex was unphosphorylated to prevent dimerization. The repeat unit was mixed with cap DNA (cap/repeat molar ratio of 1:20) and T4 DNA ligase (400 units) and incubated at 16 °C for 16 h. The head-to-tail ligated and capped concatemers were purified from preparative 2.5% agarose gels by using the QIAEX II gel-extraction kit procedure (Qiagen, Valencia, CA). The concatemers (∼10 pmol) were ligated into a recipient vector (100−150 fmol) prepared by digestion of the pT7-L15 plasmid with *Ava*I and *Mlu*I (Figure 2A). The ligated products were transformed into *E. coli* Sure2 cells (Stratagene, La Jolla, CA), to prevent corruption of the repetitive genes by recombination. The constructs were screened by *Msc*I and *Mlu*I digestion. Despite repeated attempts, L85 was not formed by this procedure and it was eventually produced by limited digestion of L105 with *Ava*I (0.2 units/μg DNA, 37 °C, 1 h), followed by purification of the concatemeric 8-mer and its ligation into the recipient vector (100−150 fmol of the pT7-L15 plasmid cut with *Ava*I and *Mlu*I) in the presence of cap DNA (2 pmol).

All DNA ligation reactions were performed with 400 units of T4 DNA ligase (New England BioLabs, Beverly, MA) for 16 h at 22 °C in 20 μL buffer, unless otherwise indicated. DNA was sequenced by Lone Star Labs (Houston, TX). Synthetic oligonucleotides were produced by Integrated DNA Technologies (Coralville, IA). The restriction enzymes and DNA-modifying enzymes were from New England BioLabs (Beverly, MA).

In Vitro Transcription and Translation (IVTT). Radiolabeled wild-type or loop-containing αHL polypeptides were synthesized by coupled IVTT in the presence of [^{35}S]-methionine, as described previously (*13*). The IVTT mix contained premix solution, amino acids minus methionine (unless otherwise stated), S30 extract (*E. coli* T7 S30 extract System, Promega, Madison, WI) pretreated with rifampicin (20 μg/mL, final concentration in IVTT mix), [^{35}S]-methionine (10 μCi/25 μL reaction, 1200 Ci/mmol, ICN, Irvine, CA), and plasmid template (4 μL/25 μL reaction, 400 ng/μL). The IVTT mix was incubated at 37 °C for 1 h.

Oligomer Formation and Purification. Radiolabeled membrane-bound wild-type and loop-containing αHL oligomers were generated by IVTT in the presence of purified rabbit red blood cell membranes (rRBCM), as described earlier (*14*). For homooligomers (W_7, $L5_7$, $L15_7$, and $L25_7$), template DNA (1.6 μg) encoding either the wild-type αHL subunit (W), or a loop-containing αHL subunit (L5, L15, or L25) was incubated with rRBCM (5 μL, 2 mg/mL membrane protein) and IVTT components, in the presence of [^{35}S]-methionine (10 μCi) and rifampicin (20 μg/mL), in a total volume of 25 μL. After 1 h at 37 °C, membrane pellets were collected and washed twice with MBSA (10 mM MOPS at pH 7.4, 150 mM NaCl, and 1 mg/mL BSA). The washed pellet was resuspended in MBSA (40 μL), prior to the addition of 2× Laemmli sample buffer (40 μL) (*15*). A portion of the sample (20 μL) was resolved in a 5% SDS−polyacrylamide gel without heating, which dissociates the subunits. The concentration of oligomers was determined by phosphorimager analysis (Molecular Imager FX, Bio-Rad, Hercules, CA; OptiQuant, Packard Instrument, Meriden, CT), by comparison with αHL wild-type heptamer standards run in parallel (*16*). The specific radioactivity of wild-type αHL was calculated based on the assumption that the specific hemolytic activity of the monomer is 25 ng/mL (*10*). Because no additional Met codons were introduced in the mutagenesis procedure, no correction for the number of methionine residues was required. Autoradiographs or phosphorimages were generally obtained after overnight exposure. For L25 homoheptamers, the gels were exposed for 21 and 2 days for autoradiograms and phosphorimages, respectively.

To obtain heterooligomers, loop-containing αHL subunits (L5, L15, or L25) were co-translated with wild-type subunits (W) in the presence of [^{35}S]methionine and rRBCM. The IVTT reactions were initiated with various molar ratios of template DNAs (W/L = 4:0, 3:1, 1:1, 1:3, and 0:4). The resulting membrane-bound heterooligomers were recovered, solubilized, and separated by electrophoresis as described for the homooligomers. For αHL subunits containing longer loops (L35, L45, L55, L65, L75, L85, L95, L105, L145, and L215), a 1:1 molar ratio of W/L DNA templates was used.

For αHL pores used in bilayer experiments, a complete amino acid mix was used in the presence of [^{35}S]methionine to increase the yield of protein synthesis (*14*). To make heteromers, a 1:1 ratio of W and L subunit templates was used, except in the case of $L25_6W_1$, when the W/L ratio was 1:3. IVTT reaction mixes were incubated at 37 °C for 1 h, in the presence of rRBCM. The solubilized membrane pellet was immediately separated in a preparative 5% SDS−polyacrylamide gel at 50 V for 16 h, with 0.1 mM Na thioglycolate in the cathode buffer. The gels were vacuum-dried at room temperature without fixing and exposed to X-ray film. Bands were excised from the gel by using the autoradiograph as a template. After rehydration, gel slices were crushed and soaked in water (500 μL) for 6−8 h. The suspension was then filtered to remove gel debris by using a cellulose acetate spin filter (Rainin, Woburn, MA). The filtrates were stored at −80 °C until required.

To check the purity of the heteromeric forms, $L25_6W_1$, $L35_4W_3$, $L85_1W_6$, $L105_1W_6$, $L145_1W_6$, and $L215_1W_6$, the gels from which they had been cut were autoradiographed again to make sure the correct material had been removed and a second SDS−polyacrylamide gel was run after the samples had been heated in Laemmli sample buffer to release the constituent monomers. The ratio of the subunits was determined by phosphorimager analysis and in all cases was in accordance with the expected result. For both the homomeric and heteromeric pores, three separate batches were prepared for each example, from each of which at least one single-channel recording was made.

Limited Proteolysis. Membrane-bound loop-containing αHL pores were prepared in two IVTT reactions (25 μL each). After 1 h at 37 °C, the combined membrane pellets were resuspended in MBSA (40 μL) and divided into four portions (9 μL each). Proteinase K (Roche Applied Science, Indianapolis, IN) solutions were prepared by dilution of a thawed enzyme stock (10 mg/mL in water) and used immediately. Water or diluted enzyme solutions were added to the samples to give final proteinase K concentrations of 0, 5, 50, and 500 μg/mL. After 5 min at 22 °C, the reactions were stopped by treatment with phenylmethylsulfonyl fluoride (2 mM final, Roche Applied Science, Indianapolis, IN) for 5 min at 22 °C, followed by the addition of 2× gel-loading buffer. The samples were immediately resolved by either 5 or 10% SDS−polyacrylamide gel electrophoresis, without prior heating. The extent of proteolysis was measured either by OptiQuant software (Packard Instrument, Meriden, CT) from phosphorimages or with ImageJ software (http://rsb.info.nih.gov/ij/, NIH, Bethesda, MD) for autoradiographs.

Thermal Stability Assay. Radiolabeled heteromeric loop-containing αHL oligomers (L5/W, L15/W, and L25/W) were synthesized by co-translation of the wild-type αHL polypeptide (W) and loop-containing αHL polypeptides (L) in the presence of [^{35}S]methionine and rRBCM. The washed membrane pellets obtained from translations with various molar ratios of templates (W/L = 4:0, 3:1, 1:1, 1:3, and 0:4) were resuspended in 20 μL of MBSA each and then pooled. An equal volume of 2× Laemmli buffer was added to the pooled mix, which was then divided into five portions (40 μL each). Each sample was overlaid with mineral oil to prevent evaporation. The samples were incubated at 22, 56, 59, 62, or 65 °C for 5 min in a Robocycler (Stratagene, La Jolla, CA). The treated samples were immediately separated by electrophoresis in 5% SDS−polyacrylamide gels, followed by autoradiography.

The radiolabeled homomeric loop-containing αHL oligomers (W_7, $L5_7$, $L15_7$, and $L25_7$) were each synthesized in four IVTT reactions (25 μL each) in the presence of [^{35}S]-methionine and rRBCM. The washed membrane pellets were resuspended and pooled in 100 μL of MBSA, followed by the addition of an equal volume of 2× Laemmli sample buffer. The solutions were divided into five tubes (40 μL each) and incubated at 22, 47, 50, 53, or 56 °C for 5 min. Each sample was overlaid with mineral oil to prevent evaporation. The samples were separated by electrophoresis in 5% SDS−polyacrylamide gels, followed by autoradiography.

Single-Channel Recording. Single-channel current recordings were performed with planar lipid bilayers generated by the method of Montal and Mueller (*17*). Briefly, a 25-μm-thick Teflon film (Goodfellow Corporation, Malvern, PA) containing a 100−150-μm-diameter orifice separated the cis and trans compartments of the recording apparatus. The aperture was pretreated with 10% (v/v) hexadecane in highly pure *n*-pentane (Burdick and Jackson, Allied Signal Inc., Muskegon, MI). 1,2-Diphytanoyl-*sn*-glycerophosphatidylcholine (Avanti Polar Lipids, Birmingham, AL) in pentane was added to both compartments, which contained 2 M NaCl and 10 mM MOPS at pH 7.4 (Fluka Chemical Co., Milwaukee, WI). After evaporation of the solvent, the solutions in both compartments were slowly elevated above the aperture to form a lipid bilayer across it. Purified heptameric αHL pores (0.7−3.2 ng/mL final concentration) were added to the cis compartment. A potential difference was applied across the bilayer with Ag/AgCl electrodes in 1.5% agarose (Bio-Rad, Hercules, CA) containing 3 M KCl. The cis chamber was at ground, and a positive potential indicates a higher potential in the trans chamber. After a single pore appeared in the bilayer, the current was recorded by using a patch clamp amplifier, Dagan 3900A (Dagan Co., Minneapolis, MN). The signals were stored on a DAS-75 data recorder (Dagan Co.). After filtering with a low-pass Bessel filter (Model 900, Frequency Devices, Haverhill, MA) with a 10 kHz cutoff frequency, the signals were acquired at 3−20 μs sampling intervals with a personal computer by using a Digidata 1200A or 1322 A/D board and Clampex 8.0 software (Axon Instruments, Union City, CA). The magnitudes of the recorded currents were determined from all-point histograms using Clampfit 9.2 (Axon Instruments, Union City, CA). The duration and frequency of substates were determined with Fetchan and PSTAT in the Clampex 8.0 package. The data are displayed in Origin 6.2 (Microcal Software Inc., Northampton, MA).

Molecular Models and Computations. The representations of the αHL pore were generated with SPOCK 6.3 (*18*) and Swiss-Model (*19*). The volume of the central cavity and the loop were calculated by using SPOCK. To determine the volume of the central cavity in the lumen of the αHL pore, an enclosed surface was required. Therefore, the top and bottom openings of the cavity were blocked by placing solid planes parallel to the rings formed by the C_α atoms of Lys-8 and Lys-147. The solvent-accessible volume and the molecular surface volume of the cavity were then computed by SPOCK. A probe of 1.4 Å radius was used to estimate the solvent-accessible volume. The software cannot compute the volume of the cavity directly, because of its large size. To overcome this, two additional planes were placed parallel to the 7-fold axis of the pore. These planes isolate a "slice" of the cavity equal to one-seventh of the total volume. The volume of the slice was adjusted to account for the volume of the bounding plane. The total cavity volume was then calculated by multiplying the volume of the slice by seven.

To determine the loop volume, a model of the L25 loop was built with Swiss-Model. Again, the molecular volume and the solvent-accessible volume were calculated by SPOCK, the latter with a probe radius of 1.4 Å. The closed-packed volume of an L25 loop was calculated from the sum of the mean residue volumes of Gly and Ser according to Harpaz et al. (*20*). The total volume of seven loops was obtained by multiplying each L25 loop volume by seven.

RESULTS

Mutant αHL Genes Encoding Gly/Ser Loops. The peptide bond upstream from position 106 in αHL was selected as the point of insertion for Gly/Ser concatemer sequences based on structural information and previous mutagenesis studies (*5*, *21*). Optimally, the polypeptide chain adjacent to the insertion position should be exposed to the solvent in both the monomeric and heptameric states of αHL for minimum perturbation of assembly and the structure of the pore. In the heptameric pore, the side chain of the wild-type residue Ser-106 is facing toward the water-filled lumen (*5*). The Gln-105 side chain of the staphylococcal leukocidin F monomer and the Lys-99 side chain of the leukocidin S monomer, which correspond to residue Ser-106 in αHL, are exposed to the solvent as well (*22*−*24*). Additionally, in the αHL pore, Ser-106 is located near the widest region of the cavity, again facilitating polypeptide insertion (Figure 1). In contrast, the side chain of the upstream residue, Asn-105, is partly buried in the αHL heptamer. Nevertheless, the overall perturbation of the structure upon loop insertion between residues 105 and 106 is tolerable as demonstrated here. In previous work, a PEG chain had been attached at position 106. Heptamers containing a single PEG chain could be assembled, but those with more than one failed to form (*7*). The cavity can also accommodate DNA oligonucleotides attached at a different site (*25*−*27*).

Glycine and serine residues are useful amino acids for the construction of linkers (loops) between domains. The hydrophilic serine side chain allows hydrogen bonding to solvent water and glycine provides the necessary flexibility (*28*, *29*). To generate the first loop-containing αHL mutant, L15, a synthetic oligonucleotide encoding PRN*GGGSGS-GSGGSGSSG*SIDTKEYA (the exogenous Gly/Ser-rich sequence is in italic) was inserted into pT7-WM102 from which a small fragment had been removed with *Msc*I and *Mlu*I (Figure 2A). The resulting plasmid, pT7-L15, was designed to generate both the repeat unit and the vector for other loop-containing αHL genes (Figure 2A).

The WM102 αHL gene in the originating plasmid, pT7-WM102, contains the mutations Tyr-102→Trp and Met-113→Ala to accommodate the *Msc*I and *Mlu*I restriction sites. During the construction of pT7-WM102, a fortuitous mutation occurred, Lys-288→Glu. In the pore, position 288 is located at the top of the cap domain (Figure 1), in the vicinity of three glutamates (Glu-287, Glu-289, and Glu-290). The Lys-288→Glu mutation generated a shift to a more rapid electrophoretic mobility in the assembled pores that is of the same magnitude as the shift seen with oligo-aspartate-tailed αHL subunits (*27*). Therefore, the mutation allowed the separation of loop-containing αHL oligomers from each other and from wild-type oligomers, without additional mutagenesis or chemical modification (Figure 2B). The unitary conductance of pores formed from Y102W/M113A/K288E (WM102) and the specific hemolytic activity of the mutant on rabbit red blood cells were similar to the wild-type values (data not shown).

Additional loop-containing subunits were designated L(10*n* + 5), where *n* is the number of repeat units and 10*n* + 5 is the total number of residues in the loop (e.g., 25 in L25). There are several different approaches for generating genes with repeat sequences (*30*, *31*). In the present work, we used a type-I endonuclease (*Ava*I) to generate nonpalindromic cohesive ends on the repeat units for one-step unidirectional concatemerization (*11*, *12*) and a nonphosphorylated cap DNA to control the average length of the concatemers (Figure 2A). The cap DNA encodes *G*SIDTKEYA, where the initial glycine is in the last repeat of the loop and the remaining residues form the sequence 106−113 of the wild-type αHL polypeptide. The *Ava*I site encodes glycine or serine; therefore, only these desired amino acid residues were introduced into the final constructs. Besides terminating concatemerization, the cap DNA provides an *Mlu*I half-site for directional cloning. The recipient vector was prepared by digesting the pT7-L15 plasmid with *Ava*I and *Mlu*I (Figure 2A). The 30-bp repeat unit was obtained by digesting the pT7-L15 with *Ava*I followed by preparative polyacrylamide gel electrophoresis. Self-ligation of the purified repeat unit with T4 DNA ligase in the presence of cap DNA generated the desired concatemers, which were gel-purified and ligated to the recipient vector. With a 1:20 molar ratio of cap to repeat DNA, αHL genes with up to 21 tandem repeats were generated (Figure 2A).

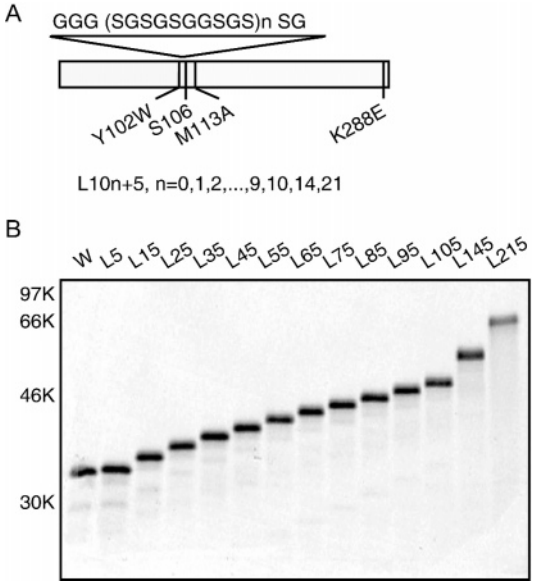

FIGURE 3: Loop-containing αHL subunits (L) used in this work. (A) Schematic of the L subunits. The Gly/Ser-rich loops were inserted before residue Ser-106. (B) Autoradiograph of an SDS−polyacrylamide gel showing monomeric L subunits (L5, L15, ..., L145, and L215) and the W subunit. Polypeptides were synthesized by IVTT in the presence of [^{35}S]methionine and resolved in a 10% gel without heating. The L subunits show decreased electrophoretic mobility that depends on the length of the loop.

The apparent molecular masses of the L subunits ranged from 33 to 59 kDa as judged by SDS−polyacrylamide gel electrophoresis; the values are somewhat higher than the calculated masses (33−49 kDa) (Figure 3). The short loop-containing mutants ($0 \leq n \leq 2$) oligomerized spontaneously after translation (data not shown). Spontaneous assembly has also been noted in mutants in which the transmembrane domain is deleted (*13*) or reversed (*14*), suggesting that the kinetic barrier to assembly is readily lowered by tinkering with the junction of the cap and stem domains.

Homooligomers Containing Short Loops Resist Limited Proteolysis and Are Stable at High Temperatures. The yield of oligomers was greater in the presence of rRBCM, which were used in subsequent experiments. To ascertain the

conformational state of the oligomers, limited proteolysis was performed. The susceptibility of $L5_7$, $L15_7$, and $L25_7$ to proteinase K digestion was compared with the susceptibility of the wild-type heptamer, W_7. If the oligomers were in a membrane-bound prepore state or a misassembled state, the amino latch or other regions of the polypeptide would be accessible and therefore sensitive to proteolysis (*22*, *32*). Wild-type pores were stable (90% undigested) at up to 500 μg/mL proteinase K as observed earlier (*13*, *16*). However, the membrane-bound oligomers containing L subunits were sensitive to proteinase K treatment even at 5 μg/mL, as visualized after electrophoresis in a 10% SDS−polyacrylamide gel (Figure 4A). Interestingly, the membrane-bound oligomers showed a more complex migration pattern in 5% gels. A fast-migrating state (band B) was sensitive to digestion by proteinase K, while a slow-migrating state (band A) was relatively resistant (Figure 4B). As the inserted loop became longer, the extent of formation of the membrane-bound SDS-resistant homoheptamers (band A) was reduced (as a fraction of W_7 formation under the same conditions: L5, 31%; L15, 8%; and L25, 4%). In the case of L5, band A was resistant to proteinase K treatment at up to 500 μg/mL (89% undigested). Bands A from the L15 or L25 subunits were partly digested under the same conditions (~70% undigested).

The fully assembled αHL pore (W_7) is stable in 2.3% SDS at up to 65 °C (*14*, *33*). The thermostability of the homoheptamers W_7, $L5_7$, $L15_7$, and $L25_7$ were compared by incubation at various temperatures (22, 47, 50, 53, and 56 °C) in electrophoresis sample buffer containing 2.3% SDS (*15*) for 5 min, followed by immediate separation in a 5% SDS−polyacrylamide gel (Figure 4C). Band A was stable at all of the temperatures tested, while band B underwent breakdown to monomers at temperatures higher than 22 °C. Further, the protein in band B failed to form pores in planar lipid bilayers (data not shown).

Formation of Heteroheptameric Pores with Short Loops ($n \leq 2$). To form heteromeric pores, L subunits were cotranslated with W subunits at various ratios in the presence of rRBCM. The K288E mutation resided only in the L subunits and generated pores of increased electrophoretic mobility, with similar gel shifts to those observed with αHL pores containing subunits with four aspartate residues at the C terminus (*27*). For each W/L combination, we identified 9 bands upon electrophoresis (Figure 5A). As seen with the homomers, the fastest migrating band, band B, was sensitive to digestion by proteinase K and was unstable above room temperature. As shown above, band B may comprise misfolded and/or misassembled pores, as reflected by proteolysis, thermal stability, and electrical recording data. Therefore, band B was not investigated further. Band A was separated into a ladder of eight species, each stepwise shift in electrophoretic mobility corresponding to the incorporation of one L subunit into the αHL oligomer. The results indicate that the homooligomers formed by L5, L15, and L25 are indeed heptamers and that all possible combinations of W and L subunits can associate (Figure 5B). In a control experiment, heteromers formed from W subunits and subunits obtained by IVTT of pT7-WM102 (containing the gene for Y102W/M113A/K288E with no encoded loop) were resolved in a 5% gel. Eight bands were again observed, in this case without a band B species (Figure 2B). The band A components for L5, L15, and L25 (the presumed homoheptamers) comigrated with homoheptamers of the WM102 protein. The wild-type homoheptamer W_7 comigrated with the heptamer formed from WM102 in which the Lys-288→Glu mutation had been reverted (Figure 2B).

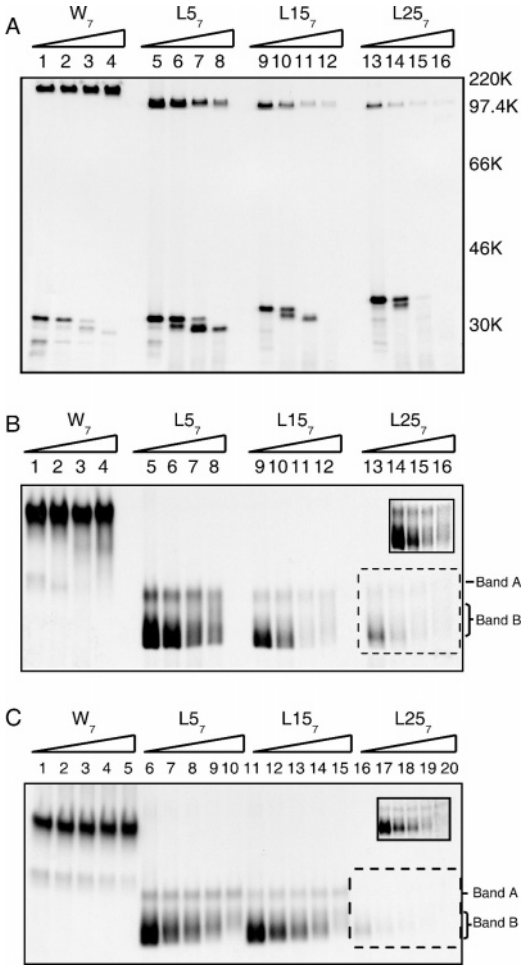

FIGURE 4: Limited proteolysis and thermal stability of homooligomers. (A and B) W_7, $L5_7$, $L15_7$, and $L25_7$ were treated with proteinase K for 5 min at 22 °C. The homooligomers were prepared by IVTT in the presence of rRBCM. The final concentrations of proteinase K were 0 μg/mL (lanes 1, 5, 9, and 13), 5 μg/mL (lanes 2, 6, 10, and 14), 50 μg/mL (lanes 3, 7, 11, and 15), and 500 μg/mL (lanes 4, 8, 12, and 16). The proteolyzed samples were resolved in either 10% (A) or 5% (B) SDS−polyacrylamide gels without prior heating. The inset in B shows an autoradiograph with a longer exposure (21 days) of lanes 13−16. The two species of oligomers observed in 5% gels are designated band A and band B. (C) Homoheptamers (W_7, $L5_7$, $L15_7$, and $L25_7$) were synthesized by IVTT in the presence of rRBCM (4 reactions, 37 °C, 1 h, 100 μL total). The washed membranes were resuspended in MBSA buffer (100 μL) followed by the addition of 2× Laemmli sample buffer (100 μL). The solution was then divided into five portions (40 μL) and incubated with a mineral oil overlay at various temperatures for 5 min. The samples were immediately resolved in a 5% SDS−polyacrylamide gel. Lanes 1, 6, 11, and 16, 22 °C; lanes 2, 7, 12, and 17, 47 °C; lanes 3, 8, 13, and 18, 50 °C; lanes 4, 9, 14, and 19, 53 °C; and lanes 5, 10, 15, and 20, 56 °C. The inset shows an autoradiograph with a longer exposure (21 days) of lanes 16−20.

Heterooligomers Containing Short Loops Are Stable at High Temperatures. Heteromers made with wild-type subunits and loop-containing subunits (L5/W, L15/W, and L25/W) showed similar stability regardless of the length of the inserted loop (Figure 5C). In contrast, the number of loops in a pore did affect its stability: heteromers with six L

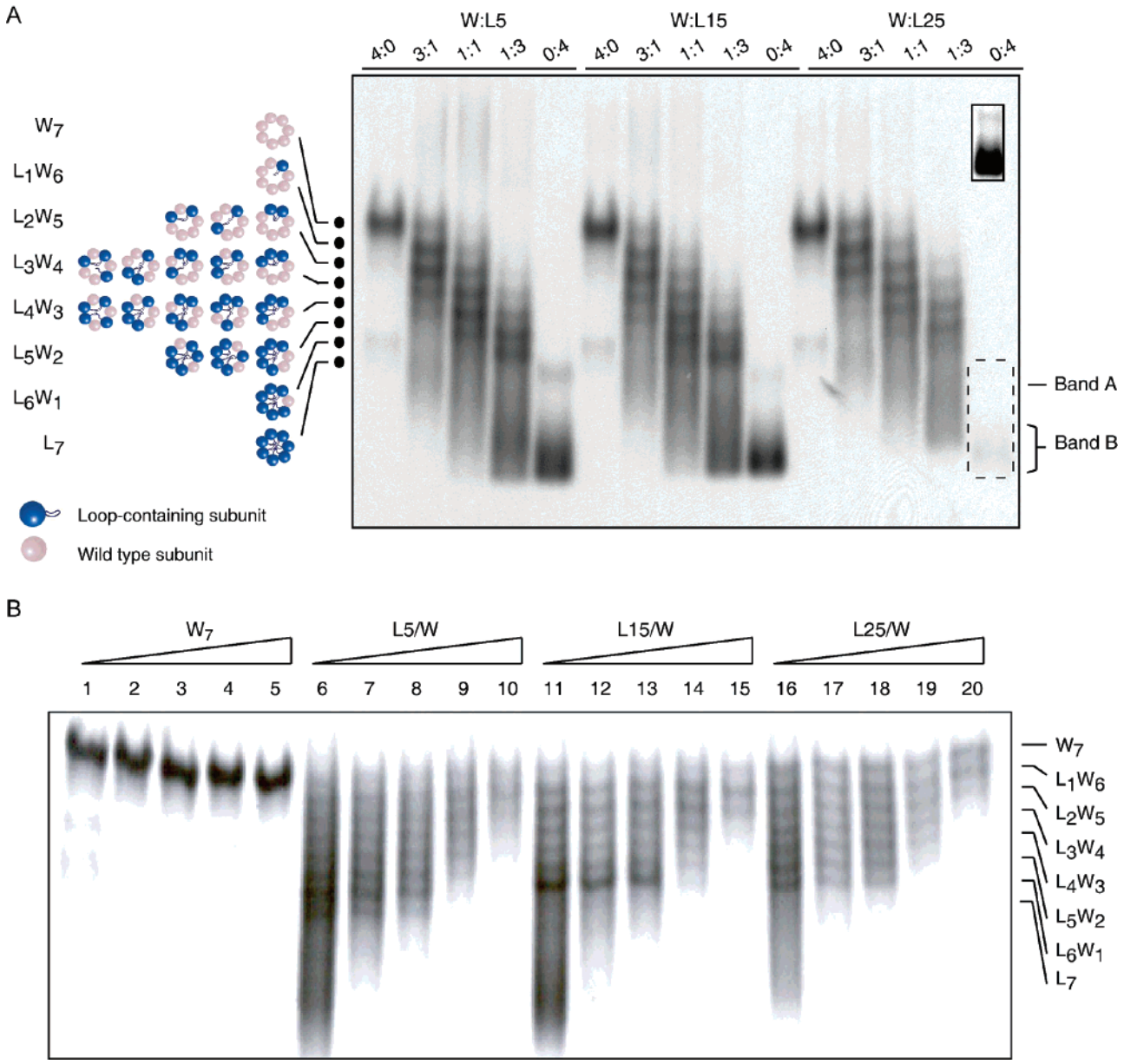

FIGURE 5: Assembly of loop-containing heterooligomeric αHL pores and their thermal stability. (A) Separation by SDS−polyacrylamide gel electrophoresis of heteromers formed from the W subunit and L subunits (L5, L15, and L25). [^{35}S]Methionine-labeled W and L subunits were synthesized and assembled into heteromers by IVTT in the presence of rRBCM. L5, L15, and L25 DNA templates were mixed with wild-type DNA template (W) in the ratios indicated above the lanes. The washed membranes were solubilized in MBSA buffer (40 μL), mixed with an equal volume of 2× Laemmli sample buffer, and subjected to electrophoresis without heating. The autoradiogram shows the electrophoretic ladders generated by the Lys-288→Glu mutation in the L subunits. The magnitude of the shift toward greater mobility depends on the number of L subunits in an oligomer. The black dots show the eight bands, indicative of a heptamer, that were formed in addition to band B. The inset shows an autoradiogram with a longer exposure (21 days) of the boxed region. A graphic representation of the heteromers is given on the left. All possible permutations of L subunit and W subunits are illustrated. The various permutations of each combination are not separated. (B) Heteroheptamers (L5/W, L15/W, and L25/W) were obtained by co-translation (37 °C, 1 h) from the W and L subunit DNA templates (L5, L15, or L25) in various ratios (W/L = 4:0, 3:1, 1:1, 1:3, and 0:4) in the presence of rRBCM. The oligomers obtained at the different ratios were pooled and treated at various temperatures as described in Figure 4C. The samples were resolved in a 5% SDS−polyacrylamide gel. Lanes 1, 6, 11, and 16, 22 °C; lanes 2, 7, 12, and 17, 56 °C; lanes 3, 8, 13, and 18, 59 °C; lanes 4, 9, 14, and 19, 62 °C; lanes 5, 10, 15, and 20, 65 °C.

subunits [$L(10n + 5)_6W_1$, $n = 0, 1, 2$] were stable at up to ~60 °C; heteromers with three to five L subunits [$L(10n + 5)_{3-5}W_{4-2}$, $n = 0, 1, 2$] were stable at up to ~63 °C, while $L(10n + 5)_1W_6$, and $L(10n + 5)_2W_5$, ($n = 0, 1, 2$) were as stable as the W_7 pore (Figure 5C).

Subunits Containing Longer Loops Form Heteroheptamers with Wild-Type αHL Subunits, but Not Homoheptamers. To explore the capacity of the cavity of αHL for L subunits with longer loops ($n \geq 3$), additional heteromers were assembled with W subunits (Figure 6A). For short loops ($0 \leq n \leq 2$), pores with seven L subunits could form (Figure 5A). However, if the loops were longer than 25 residues ($n \geq 3$), the L subunits could not assemble by themselves (data not shown), but they did form heteromers with W subunits (Figure 6A). Five subunits of L35 ($n = 3$) were able to assemble with two W subunits, while up to three subunits of L45 ($n = 4$) were incorporated into heptamers. For longer loops ($n = 5$ or 6), up to two L subunits were tolerated. For

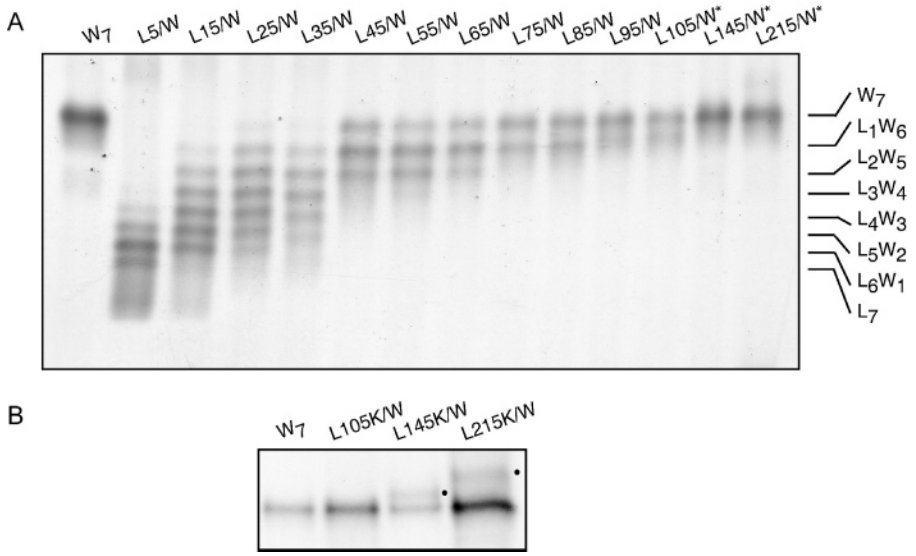

FIGURE 6: Maximum allowed number of loops of various lengths in the heteroheptameric pores. (A) Heteroheptamers (L5/W, L15/W, ..., L145/W, and L215/W) were synthesized by IVTT in the presence of rRBCM for 1 h at 37 °C. The templates were mixtures of W subunit DNA and L subunit DNA in a 1:1 ratio. Membrane-bound oligomers were resolved in 5% SDS−polyacrylamide gels without heating. The faster migrating heteromeric bands are labeled on the right. In the cases of L105/W, L145/W, and L215/W (starred lanes), the heteromers (containing one L subunit) migrate more slowly than L_1W_6 in the other lanes. (B) Heteromers formed from revertants of the Lys-288→Glu mutation (L5K/W, L15K/W, ..., L145K/W, and L215K/W) were generated by co-translation in the presence of rRBCM and resolved in a 5% gel without heating. The templates were mixtures of W subunit DNA and L(10*n* + 5)K subunit DNA in a 1:1 ratio.

loops with more than 7 repeats ($7 \leq n \leq 10$, $n = 14$ or 21), only one L subunit was incorporated. These heteromers were protease-resistant (data not shown). When higher ratios of L/W were tested (up to 6:1), no additional L subunits were incorporated.

The electrophoretic mobility of the L_1W_6 heptamers was reduced when the length of loop was longer than 95 residues; in these cases, the effect of the loop outweighed that of the Lys-288→Glu mutation. For example, $L105_1W_6$ migrated slightly more slowly than L_1W_6 for L5−L95, while $L215_1W_6$ migrated more slowly than even W_7 (Figure 6A). When the Lys-288→Glu mutation was reversed (to "E288K"), the ladders caused by the incorporation of L subunits were not observed but the decrease in electrophoretic mobility caused by the loops in $L145_1W_6$ and $L215_1W_6$ were clearly visible (Figure 6B).

Single-Channel Recordings of Loop-Containing Pores. The properties of gel-purified loop-containing oligomers were examined by planar bilayer recording in 2 M KCl and 10 mM MOPS at pH 7.4 (Figure 7). In all cases reported, a single pore inserted into the bilayer as evidenced by a single step from zero current. Unitary conductance values for $L5_7$ and $L15_7$ were 1.91 ± 0.02 nS ($N = 4$) and 1.90 ± 0.02 nS ($N = 3$), respectively, at +100 mV. Under the same conditions, the unitary conductance of W_7 was 2.18 ± 0.21 nS ($N = 8$). Similar to W_7, the currents were devoid of substates. In contrast, when the cavity was fully packed with polypeptide loops, the residual current was greatly reduced relative to W_7: $L35_4W_3$, 1.10 ± 0.04 nS ($N = 5$); $L25_6W_1$, 1.01 ± 0.15 nS ($N = 5$); and $L25_7$, 0.67 ± 0.02 nS ($N = 5$) (Figure 7).

With single long loops ($n = 8$ or 10), transient partial closures of the pore were observed at positive applied potentials but not at negative potentials (Figure 7A), similar to those seen with αHL pores with PEG chains covalently attached within the cavity (*7*). The lifetimes of the closures were 99 ± 7 μs for $L85_1W_6$ and 593 ± 63 μs for $L105_1W_6$. The unitary conductance values were 1.59 ± 0.01 and 1.72 ± 0.08 nS, respectively, for $L85_1W_6$ and $L105_1W_6$, and the magnitude of the blockade in the closed state was ∼1.53 nS in both cases. Unlike $L85_1W_6$ and $L105_1W_6$, $L145_1W_6$ and $L215_1W_6$, the pores with the longest single loops, exhibited high unitary conductance values and no closures, similar to W_7, $L5_7$, and $L15_7$. The conductance values were $L145_1W_6$ = 2.06 ± 0.11 nS ($N = 5$) and $L215_1W_6$ = 1.92 ± 0.04 nS ($N = 5$).

DISCUSSION

Here, we describe an unusual piece of protein engineering in which an internal cavity within a transmembrane protein pore has been filled with additional polypeptide sequences. The engineered heptameric pores contained either seven small polypeptide loops or a smaller number of large loops. The pores were stable as judged by protease sensitivity and thermolability and functional as judged by their ability to form pores in planar lipid bilayers.

$L25_7$ was the homomeric pore that contained the largest amount of foreign sequence, 175 residues. The electrophoretic mobility of $L25_7$ was identical to that of W_7 (e.g., Figure 6B), suggesting that its hydrodynamic properties are unaltered and, therefore, that the additional polypeptide chains are contained within the protein. The conductance of $L25_7$ was 31% of that of W_7; therefore, hydrated ions are still free to pass through it (Figure 7). The current passing through the pore exhibited excess noise, which might arise from movement of the loops near the constriction or from destabilization of the structure (Figure 7).

The molecular surface volume of the cavity in the cap domain is 39 500 Å^3, and the accessible volume is 32 600 Å^3. The latter was computed with a rolling sphere of 1.4 Å radius and therefore excludes the volume taken up by approximately a half layer of water molecules on the surface of the cavity (*34*). The molecular surface and accessible

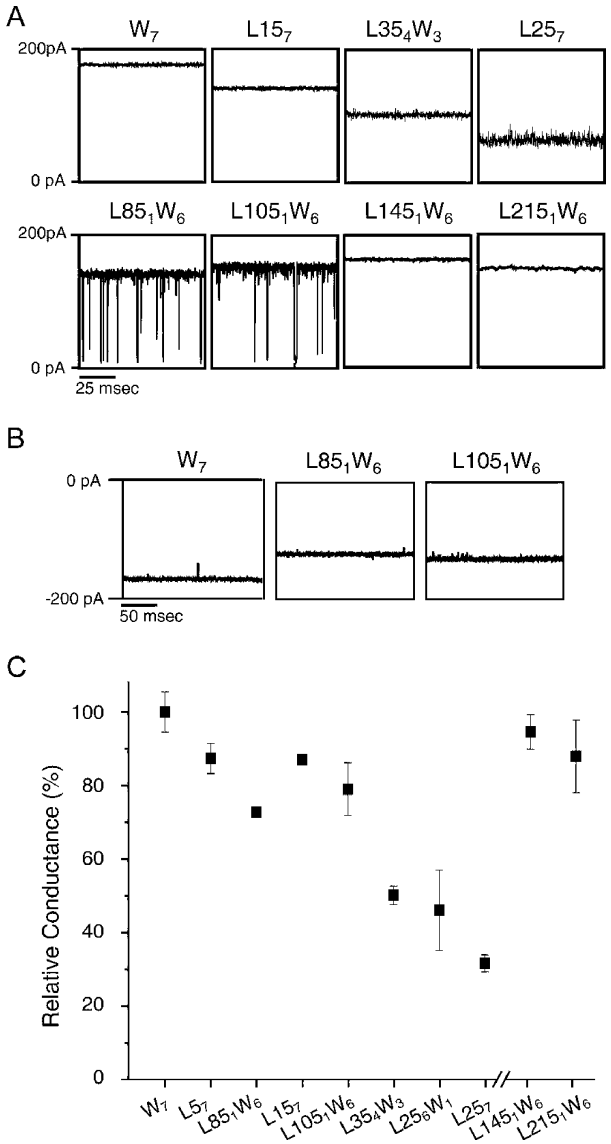

FIGURE 7: Single-channel recordings of heteromeric pores containing Gly/Ser loops. (A) Single-channel recordings performed at +100 mV in 2 M KCl and 10 mM MOPS at pH 7.4. The currents were filtered at 10 kHz. Each heteromer was obtained by IVTT (37 °C, 1 h) in the presence of rRBCM and purified from a preparative 5% gel. (B) Traces of W_7, $L85_1W_6$, and $L105_1W_6$ at −100 mV. The conditions were the same as in A. (C) Single-channel conductance values were determined and expressed as a percentage of the W_7 conductance. Error bars indicate the standard deviations from the mean ($N = 8$ for W_7, and $N = 3-5$ for the rest). The recording conditions are the same as in A. The total number of inserted amino acids in the examined pores increases along the *x* axis, except for $L145_1W_6$ and $L215_1W_6$.

volumes of seven L25 loops, each including 14 Gly and 11 Ser residues, are 8300 and 23 200 Å^3, respectively. The latter value assumes that each loop is separately and fully hydrated. The close packed volume of the Gly and Ser residues is 13 500 Å^3 (*20*), which suggest that the modeling software underestimates the molecular surface volume of the loop. Therefore, the central cavity of the αHL pore can readily accommodate seven L25 loops as shown experimentally in the present work. In contrast, seven L35 loops would be a tight fit when fully hydrated. A high degree of hydration is in keeping with the ability of the $L25_7$ pore to conduct ions.

The accessible volumes determined with SPOCK of 22 proteins (1CHH, 1A2P, 2PYP, 132L, 1A29, 1A2T, 1D1M, 1F18, 142L, 1CV8, 1AHN, 1FAJ, 1WBA, 1BG7, 1KHI, 1L4U, 1JUV, 1ATK, 1AQ7, 1C4F, 1AG1, and 1DUI) containing 108−275 residues were plotted versus the number of residues. From a linear fit, the number of residues corresponding to an accessible volume of 32 600 Å^3, which might just fit within the hydrated cavity, is 176 (not shown). In these cases, the mean residue volume is far greater than that of Gly or Ser. The mean close-packed volumes of seven of these proteins, with 174−176 residues (1CV8, 1AHN, 1FAJ, 1WBA, 1BG7, 1KHI, and 1L4U), is 19 700 Å^3, as calculated according to Harpaz et al. (*20*).

Only one copy of the largest loops (more than 75 amino acids) could be incorporated per heptamer, which is reminiscent of attempts to place covalently attached PEG chains within the pore (*7*). For example, only one copy of a 5-kDa PEG could be placed within the cap domain. Pores with more than one PEG chain failed to assemble. The unitary conductance of pores of the form L_1W_6 did not differ greatly from W_7. For example, the conductance of $L105_1W_6$ was 79% of W_7. Interestingly, $L105_1W_6$ and similar pores ($n = 8-10$), exhibited transient blockades (Figure 7A), suggesting that the loop was able to move into the constriction and almost completely block the pore. When the loop was larger still ($n = 14$ and 21), no blockades were seen ($L145_1W_6$ and $L215_1W_6$, Figure 7A), suggesting that in these cases the loop is extruded through the cis entrance into the medium in keeping with the altered electrophoretic mobility of these pores. In the cases of $L145_1W_6$ and $L215_1W_6$ but not $L105_1W_6$, the electrophoretic mobility was significantly reduced compared to W_7 (Figure 6B). This finding is again reminiscent of the properties of pores containing covalently attached PEG chains. For example, a pore containing a 3.4-kDa chain, terminated at the free end with biotin, comigrated with the unmodified heptamer (W_7) and exhibited numerous spikes toward lower conductance, similar to $L105_1W_6$. When the PEG chain was captured in the cis compartment with streptavidin, the current became quiet, like that of $L215_1W_6$ (*8*). The volume calculations suggest that hydrated L145 and L215 loops might be accommodated within the cavity, and the fact that they are extruded suggests that confinement bears a high entropic cost (*35*).

Besides its intrinsic interest as an engineering feat, the ability to place foreign sequences within the cavity of the αHL pore has implications in biotechnology. Engineered αHL pores have been developed as components of stochastic sensors. In this approach, the ionic current flowing through a single pore is monitored. Events corresponding to the binding of individual analyte molecules to the pore can be detected, permitting the identification and quantification of a wide variety of analytes (*1*). Using the developments reported here, polypeptide loops might be placed within the cavity that respond to small analytes, such as divalent metal ions (*36*). Loops that respond to physical conditions such as the temperature (*37*) might also be incorporated. Longer loops that extend outside the cavity might be useful for sensing. We have already shown that the movement of a PEG chain of 3.4 kDa, attached within the pore, responds to the binding of a protein analyte to the free end of the chain (*8*). The altered mobility of the polymer is evident in current recordings from single pores. It should then be possible to introduce binding sites for analytes within subunits such as L105, which produce current spikes when

incorporated into heteromeric pores (Figure 7). The binding sites could be peptide epitopes or small molecules attached to a central cysteine in the loop. If the loop responds to macromolecular analytes in the same way as the PEG chain, we would expect the spikes to be dampened while an analyte is bound.

On the basis of the calculated volume of the cavity and the feasibility demonstrated by this work, it is possible that a small folded protein might be incorporated within the αHL pore. Conceivably, the protein could be functional, an enzyme for example. In the long term, it might be possible to convert a substrate to product during transit through the pore. This combination of transformation and transport would be of obvious use in manufacturing and decontamination.

ACKNOWLEDGMENT

We thank Dr. Sean Conlan for help with molecular modeling and the carbon plane coordinates.

REFERENCES

1. Bayley, H., and Cremer, P. S. (2001) Stochastic sensors inspired by biology, *Nature 413*, 226−230.
2. Eroglu, A., Russo, M. J., Bieganski, R., Fowler, A., Cheley, S., Bayley, H., and Toner, M. (2000) Intracellular trehalose improves the survival of cryopreserved mammalian cells, *Nat. Biotechnol. 18*, 163−167.
3. Shin, S. H., Luchian, T., Cheley, S., Braha, O., and Bayley, H. (2002) Kinetics of a reversible covalent-bond-forming reaction observed at the single-molecule level, *Angew. Chem. Int. Ed. 41*, 3707−3709.
4. Montoya, M., and Gouaux, E. (2003) *β*-Barrel membrane protein folding and structure viewed through the lens of α-hemolysin, *Biochim. Biophys. Acta 1609*, 19−27.
5. Song, L., Hobaugh, M. R., Shustak, C., Cheley, S., Bayley, H., and Gouaux, J. E. (1996) Structure of staphylococcal α-hemolysin, a heptameric transmembrane pore, *Science 274*, 1859−1866.
6. Galdiero, S., and Gouaux, E. (2004) High-resolution crystallographic studies of α-hemolysin−phospholipid complexes define heptamer−lipid head group interactions: Implication for understanding protein−lipid interactions, *Protein Sci. 13*, 1503−1511.
7. Howorka, S., Movileanu, L., Lu, X., Magnon, M., Cheley, S., Braha, O., and Bayley, H. (2000) A protein pore with a single polymer chain tethered within the lumen, *J. Am. Chem. Soc. 122*, 2411−2416.
8. Movileanu, L., Howorka, S., Braha, O., and Bayley, H. (2000) Detecting protein analytes that modulate transmembrane movement of a polymer chain within a single protein pore, *Nat. Biotechnol. 18*, 1091−1095.
9. Howorka, S., and Bayley, H. (1998) Improved protocol for high-throughput cysteine scanning mutagenesis, *BioTechniques 25*, 766−772.
10. Walker, B., Krishnasastry, M., Zorn, L., Kasianowicz, J., and Bayley, H. (1992) Functional expression of the α-hemolysin of *Staphylococcus aureus* in intact *Escherichia coli* and in cell lysates. Deletion of five C-terminal amino acids selectively impairs hemolytic activity, *J. Biol. Chem. 267*, 10902−10909.
11. Hartley, J. L., and Gregori, T. J. (1981) Cloning multiple copies of a DNA segment, *Gene 13*, 347−353.
12. Liaw, G. J. (1994) Improved protocol for directional multimerization of a DNA fragment, *BioTechniques 17*, 668−670.
13. Cheley, S., Malghani, M. S., Song, L., Hobaugh, M., Gouaux, J. E., Yang, J., and Bayley, H. (1997) Spontaneous oligomerization of a staphylococcal α-hemolysin conformationally constrained by removal of residues that form the transmembrane *β*-barrel, *Protein Eng. 10*, 1433−1443.
14. Cheley, S., Braha, O., Lu, X., Conlan, S., and Bayley, H. (1999) A functional protein pore with a "retro" transmembrane domain, *Protein Sci. 8*, 1257−1267.
15. Laemmli, U. K. (1970) Cleavage of structural proteins during the assembly of the head of bacteriophage T4, *Nature 227*, 680−685.
16. Miles, G., Bayley, H., and Cheley, S. (2002) Properties of *Bacillus cereus* hemolysin II: a heptameric transmembrane pore, *Protein Sci 11*, 1813−1824.
17. Montal, M., and Mueller, P. (1972) Formation of bimolecular membranes from lipid monolayers and a study of their electrical properties, *Proc. Natl. Acad. Sci. U.S.A. 69*, 3561−3566.
18. Christopher, J. A. (1998) *SPOCK: The Structural Properties Observation and Calculation Kit (Program Manual)*, Center for Macromolecular Design, Texas A&M University, College Station, TX.
19. Guex, N., and Peitsch, M. C. (1997) SWISS-MODEL and the Swiss-PdbViewer: An environment for comparative protein modeling, *Electrophoresis 18*, 2714−2723.
20. Harpaz, Y., Gerstein, M., and Chothia, C. (1994) Volume changes on protein folding, *Structure 2*, 641−649.
21. Walker, B., and Bayley, H. (1995) Key residues for membrane binding, oligomerization, and pore forming activity of staphylococcal α-hemolysin identified by cysteine scanning mutagenesis and targeted chemical modification, *J. Biol. Chem. 270*, 23065−23071.
22. Olson, R., Nariya, H., Yokota, K., Kamio, Y., and Gouaux, E. (1999) Crystal structure of staphylococcal LukF delineates conformational changes accompanying formation of a transmembrane channel, *Nat. Struct. Biol. 6*, 134−140.
23. Guillet, V., Roblin, P., Werner, S., Coraiola, M., Menestrina, G., Monteil, H., Prevost, G., and Mourey, L. (2004) Crystal structure of leucotoxin S component: New insight into the staphylococcal *β*-barrel pore-forming toxins, *J. Biol. Chem. 279*, 41028−41037.
24. Pedelacq, J. D., Maveyraud, L., Prevost, G., Baba-Moussa, L., Gonzalez, A., Courcelle, E., Shepard, W., Monteil, H., Samama, J. P., and Mourey, L. (1999) The structure of a *Staphylococcus aureus* leucocidin component (LukF-PV) reveals the fold of the water-soluble species of a family of transmembrane pore-forming toxins, *Struct. Fold Des. 7*, 277−287.
25. Howorka, S., and Bayley, H. (2002) Probing distance and electrical potential within a protein pore with tethered DNA, *Biophys. J. 83*, 3202−3210.
26. Howorka, S., Movileanu, L., Braha, O., and Bayley, H. (2001) Kinetics of duplex formation for individual DNA strands within a single protein nanopore, *Proc. Natl. Acad. Sci. U.S.A. 98*, 12996−13001.
27. Howorka, S., Cheley, S., and Bayley, H. (2001) Sequence-specific detection of individual DNA strands using engineered nanopores, *Nat. Biotechnol. 19*, 636−639.
28. Huang, F., and Nau, W. M. (2003) A conformational flexibility scale for amino acids in peptides, *Angew. Chem. Int. Ed. 42*, 2269−2272.
29. George, R. A., and Heringa, J. (2002) An analysis of protein domain linkers: Their classification and role in protein folding, *Protein Eng. 15*, 871−879.
30. Blachinsky, E., Marbach, I., Cohen, R., Grably, M. R., and Engelberg, D. (2004) Procedure for controlling number of repeats, orientation, and order during cloning of oligonucleotides, *BioTechniques 36*, 933−936.
31. Wright, E. R., and Conticello, V. P. (2002) Self-assembly of block copolymers derived from elastin-mimetic polypeptide sequences, *Adv. Drug Delivery Rev. 54*, 1057−1073.
32. Walker, B., Braha, O., Cheley, S., and Bayley, H. (1995) An intermediate in the assembly of a pore-forming protein trapped with a genetically engineered switch, *Chem. Biol. 2*, 99−105.
33. Walker, B., and Bayley, H. (1995) Restoration of pore-forming activity in staphylococcal α-hemolysin by targeted chemical modification, *Protein Eng. 8*, 491−495.
34. Richards, F. M. (1977) Areas, volumes, packing, and protein structure, *Annu. Rev. Biophys. Bioeng. 6*, 151−176.
35. Movileanu, L., and Bayley, H. (2001) Partitioning of a polymer into a nanoscopic protein pore obeys a simple scaling law, *Proc. Natl. Acad. Sci. U.S.A. 98*, 10137−10141.
36. Braha, O., Walker, B., Cheley, S., Kasianowicz, J. J., Song, L., Gouaux, J. E., and Bayley, H. (1997) Designed protein pores as components for biosensors, *Chem. Biol. 4*, 497−505.
37. Yamaoka, T., Tamura, T., Seto, Y., Tada, T., Kunugi, S., and Tirrell, D. A. (2003) Mechanism for the phase transition of a genetically engineered elastin model peptide (VPGIG)40 in aqueous solution, *Biomacromolecules 4*, 1680−1685.

BI0473713